2001-03-31

Centrosome defects can account for cellular and genetic changes that characterize prostate cancer progression

German A. Pihan
University of Massachusetts Medical School

Et al.

[CANCER RESEARCH 61, 2212–2219, March 1, 2001]

Centrosome Defects Can Account for Cellular and Genetic Changes That Characterize Prostate Cancer Progression[1]

German A. Pihan,[2] Aruna Purohit, Janice Wallace, Raji Malhotra, Lance Liotta, and Stephen J. Doxsey[2]

Department of Pathology [G. A. P., J. W., R. M.] and Program in Molecular Medicine [A. P., S. J. D.], University of Massachusetts Medical School, Worcester, Massachusetts 01655, and Department of Pathology, National Cancer Institute, Bethesda, Maryland 20892 [L. L.]

ABSTRACT

Factors that determine the biological and clinical behavior of prostate cancer are largely unknown. Prostate tumor progression is characterized by changes in cellular architecture, glandular organization, and genomic composition. These features are reflected in the Gleason grade of the tumor and in the development of aneuploidy. Cellular architecture and genomic stability are controlled in part by centrosomes, organelles that organize microtubule arrays including mitotic spindles. Here we demonstrate that centrosomes are structurally and numerically abnormal in the majority of prostate carcinomas. Centrosome abnormalities increase with increasing Gleason grade and with increasing levels of genomic instability. Selective induction of centrosome abnormalities by elevating levels of the centrosome protein pericentrin in prostate epithelial cell lines reproduces many of the phenotypic characteristics of high-grade prostate carcinoma. Cells that transiently or permanently express pericentrin exhibit severe centrosome and spindle defects, cellular disorganization, genomic instability, and enhanced growth in soft agar. On the basis of these observations, we propose a model in which centrosome dysfunction contributes to the progressive loss of cellular and glandular architecture and increasing genomic instability that accompany prostate cancer progression, dissemination, and lethality.

INTRODUCTION

Prostate carcinoma is the most common gender-specific cancer in the United States, accounting for nearly one-third of all cancers affecting men (1). The lifetime risk of developing invasive prostate carcinoma in the United States is ~20% (2–5), whereas that of octogenarians based on histopathological examination of the prostate at autopsy approaches 80% (6). Despite the high incidence of prostate carcinoma, the lifetime risk of dying from the disease is much lower, currently estimated to be ~3.6% (1 of 28; Surveillance Epidemiology & End Results, NCI, 2000, personal communication). These epidemiological trends, which may intensify in the coming decades because of the aging of the Baby Boom generation and our increasing ability to recognize tumors at earlier stages, mean that 180,000 new cases of prostate cancer will be diagnosed in the coming year in the United States.

Radical prostatectomy is the most common therapy for the small group of patients with high-grade tumors. However, there currently are no sound medical facts to direct treatment of the majority of patients that present with lower grade tumors (7, 8). Because a subgroup of patients with low-grade carcinoma ultimately develop aggressive, often lethal cancers, current therapeutic recommendations are to treat all patients with an intent to cure (7, 8). Thus, the most pressing need in the management of prostate carcinoma is to develop a noninvasive test to distinguish clinically indolent (low-grade) carcinoma from potentially fatal disease (see "Discussion"; Ref. 9). This test would spare the majority of patients with indolent prostate cancer from unnecessary prostatectomy. Reducing such surgeries would result in significant cost savings in health care, decreased therapy-related morbidity, and more focused therapy on the more homogeneous group of patients with aggressive disease, where the efficacy of newer therapies could be assessed more quickly (9).

One of the best predictors of prostate cancer progression is the Gleason score, a numerical measure compiled from the two most prevalent histological Gleason grades. The Gleason grade reflects cytoarchitectural features that become increasingly aberrant with tumor progression (10, 11). Recent results indicate that the parameter with the greatest predictive power is the proportion of tumor with the highest Gleason grades (4 and 5; Ref. 12). An intimate relationship between Gleason grade, aneuploidy, and unfavorable clinical outcome has long been known (13–17). This suggests that the molecular components and subcellular structures that control cell and tissue architecture and genetic fidelity are likely to contribute to tumor progression. These parameters have the potential to dictate the clinical behavior of tumors and thus serve as predictors of aggressive cancer.

In a search for cellular elements that contribute to the constellation of cellular and genetic features found in high Gleason grade prostate carcinoma, we focused on centrosomes (18). Centrosomes are tiny cellular organelles that nucleate microtubule growth and organize the mitotic spindle for segregating chromosomes into daughter cells (reviewed in Refs. 19 and 20). As organizers of microtubules, centrosomes also play an important role in many microtubule-mediated processes, such as establishing cell shape and cell polarity, processes essential for epithelial gland organization (21–24). Centrosomes also coordinate numerous intracellular activities in part by providing docking sites for regulatory molecules, including those that control cell cycle progression, centrosome and spindle function, and cell cycle checkpoints (20, 24–29). Because high Gleason grade prostate cancer is characterized by defects in the same set of cellular processes controlled by centrosomes, we hypothesized that centrosome dysfunction may be the biological basis for these phenotypic abnormalities.

In this report, we show that centrosome defects are found in essentially all high-grade prostate cancers. Moreover, centrosome defects are present in low-grade tumors, and they increase with increasing Gleason grade and with increasing genomic instability. Artificial induction of centrosome abnormalities in cultured prostate cells by overexpression of the centrosome protein pericentrin reproduces many features of aggressive prostate cancer. We discuss our results in terms of a centrosome-mediated mechanism for tumor progression. Centrosome abnormalities in prostate cancer could be exploited to develop markers for tumor virulence and selective therapies that target tumor-specific centrosome abnormalities, thus circumventing the greatest limitation of current chemotherapy–its lack of tumor selectivity.

MATERIALS AND METHODS

Immunohistochemical Detection of Centrosomes in Archival Tissue Sections of Prostate Carcinoma. Archived cases of invasive prostate carcinoma treated by radical prostatectomy were selected from the files of the

Received 8/25/00; accepted 12/29/00.

The costs of publication of this article were defrayed in part by the payment of page charges. This article must therefore be hereby marked *advertisement* in accordance with 18 U.S.C. Section 1734 solely to indicate this fact.

[1] Supported by Grants PC970425 and PC000018 (to G. A. P. and S. J. D.) from the Department of Defense, Grant RO1 GM51994 (to S. J. D.) from the NIH, and funds from the Massachusetts Department of Public Health and Our Danny Cancer Fund (to G. A. P. and S. J. D.). S. J. D. is a recipient of an Established Investigator Award 96-276 from the American Heart Association.

[2] To whom requests for reprints should be addressed, at Department of Pathology, Room S2–141, University of Massachusetts Medical School, 55 Lake Avenue North, Worcester, MA 01655. Phone: (508) 856-4124; Fax: (508) 856-5780; E-mail: German.pihan@umassmed.edu, or Department of Molecular Medicine, University of Massachusetts Medical School, 373 Plantation Street, Worcester, MA 01605. Phone: (508) 856-1613; Fax: (508) 856-4289; E-mail: stephen.doxey@umassmed.edu.

Table 1 *Centrosome abnormalities in prostate carcinoma*

Tumor type[a]	Abnormal centrosomes[b]	
	Non-tumor epithelium[c]	Tumor epithelium
Metastatic prostate carcinoma	0/31[d]	31/31
Prostate carcinoma confined to the prostate	0/97	101/109

[a] Tumors were identified by cellular, glandular, and nuclear features in H&E-stained sections. Parallel sections were stained for pericentrin by the immunoperoxidase technique to detect centrosomes and counterstained with hematoxylin only.

[b] For all samples in this analysis, paraffin-embedded tissues were sectioned, reacted with pericentrin antibodies and immunoperoxidase methods, and examined by light microscopy. The centrosome defects in tumor tissue were statistically higher than control non-tumor glands ($P < 0.0001$, Fisher's exact test). Centrosomes were considered abnormal if they had a diameter at least twice that of centrosomes in normal prostate gland epithelium, if they were structurally abnormal (elongated), if they were present in more than two copies/cell, and if they had increased cytoplasmic and or centrosomal staining levels of the centrosome protein pericentrin (18).

[c] Non-tumor epithelium was present within the same section that contained the tumor in the majority of the cases (97 of 109).

[d] Control cells in metastatic organs included cells of that organ (lymphocytes and hematopoietic cells in lymph nodes and bone marrow) as described previously (18).

Department of Pathology of the University of Massachusetts Medical Center accrued between the months of July 1995 and June of 1997. Criteria for inclusion were availability of archival tissue blocks from which good quality histology sections could be prepared. Sections with the highest Gleason grade from each radical prostatectomy were selected because there is good indication that the highest Gleason grade is the best indicator of clinical outcome (12). We analyzed only high quality tissue sections (109 total) from radical prostatectomies with invasive carcinoma representing Gleason grades 2–5 and from metastatic prostate carcinoma (31 cases). Immunostaining for pericentrin was judged satisfactory when the characteristic single or paired centrosome pattern (30) was detected in nonneoplastic cells adjacent to the tumor (Table 1).

Immunohistochemistry for pericentrin (18) was performed on serial paraffin sections (5 μm thick) attached to positively charged glass slides (Ventana Medical Systems). The first section of each series was stained with H&E to confirm the presence and grade of the carcinoma and to map the tumor within the section. Parallel sections were processed for centrosome staining by immunohistochemistry. Sections were first heated in a microwave pressure cooker for 30 min in a solution containing 0.2 mM EDTA (18) to render

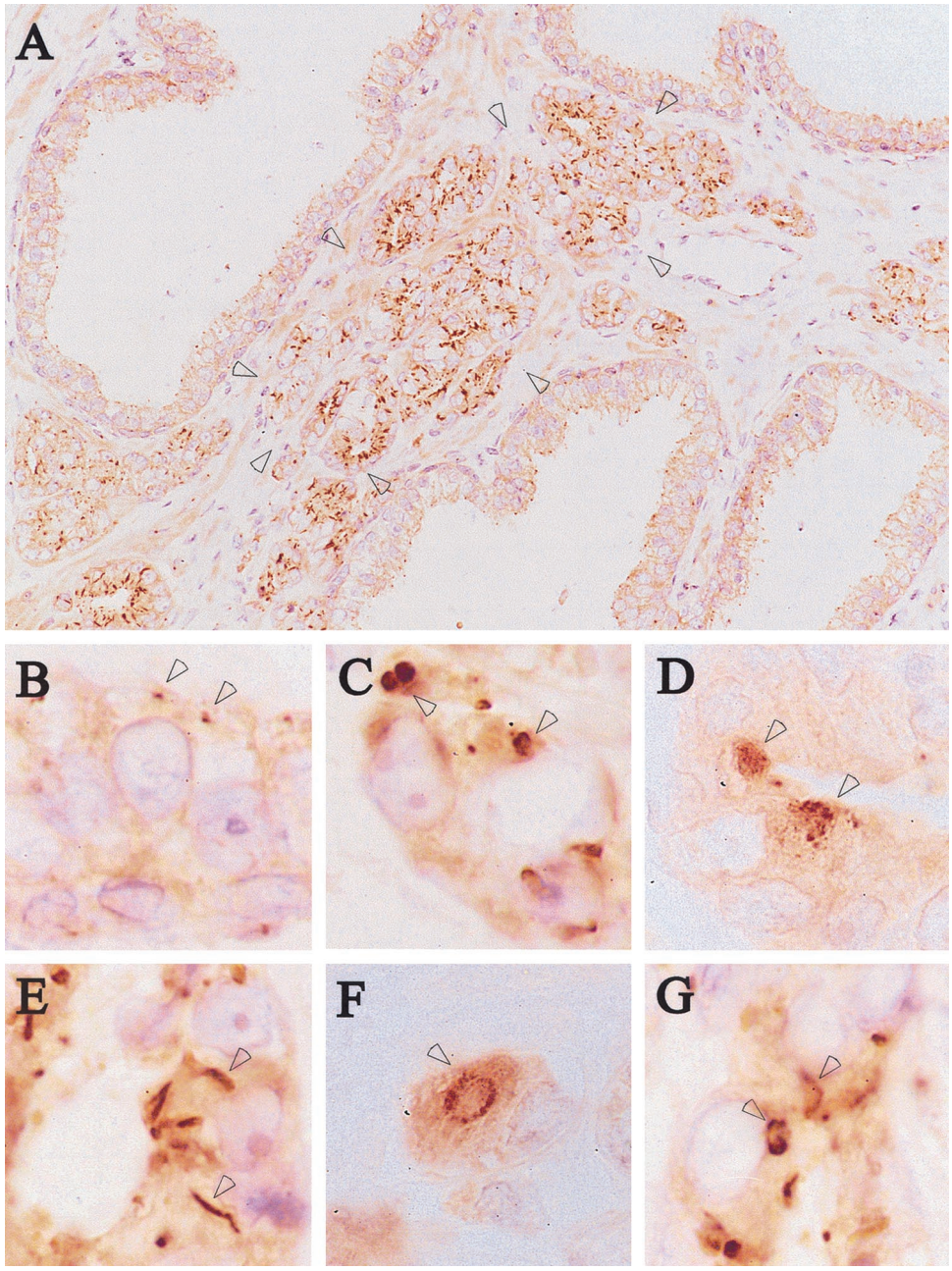

Fig. 1. Centrosome abnormalities in invasive prostate carcinoma compared with adjacent normal tissue. Sections from radical prostatectomies were stained for pericentrin (*brown*) as described in "Materials and Methods." *A*, prominent centrosome abnormalities are seen in small tumor glands (between *arrowheads*) compared with centrosomes in three large normal glands (*top left*, *top*, and *bottom right*). ×100. *B–G:* higher magnification (×1000) of centrosomes in tumor cells (*C–G*) and nontumor cells (*B*). Centrosomes in tumor cells (*arrowheads*) are larger in diameter (*C*, *G*, *arrowheads*), elongated (*E*, *arrowheads*), multiple and apparently fragmented (*D* and *F*), and contain more pericentrin (*C–G*) than control centrosomes (*arrowheads* in *B*). Most tumors had combinations of centrosome defects.

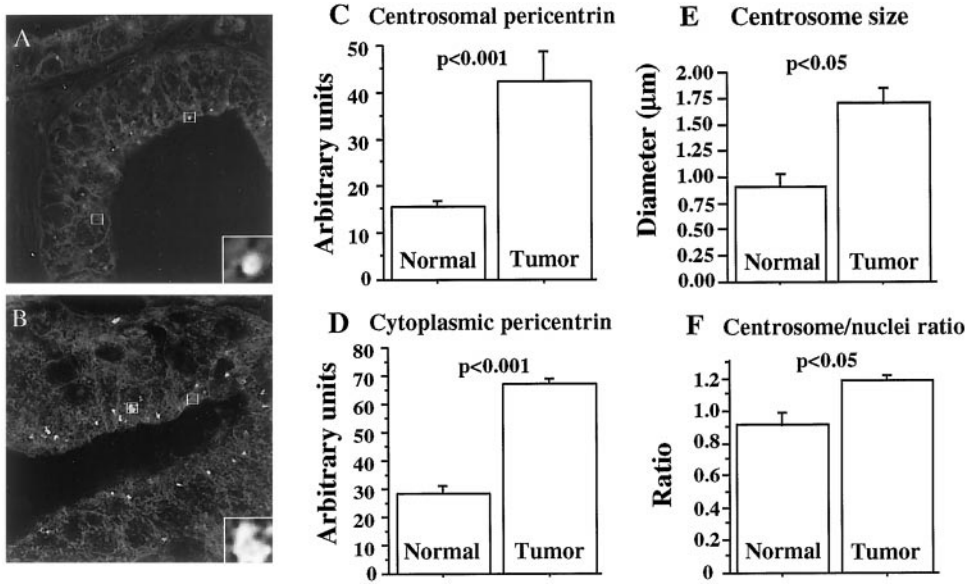

Fig. 2. Centrosome diameter and number are increased, and pericentrin levels are elevated in prostate carcinoma. Measurements from a single grade 3 prostate carcinoma are shown. *A–D*, densitometric measurements of centrosomes and cytoplasm were performed on tumor tissues and nontumor tissues as described in "Materials and Methods" (33). Immunoperoxidase reaction product was quantified by measuring translucence in *boxes* shown in *A* and *B*. *Insets* in *A* and *B*, higher magnification of centrosomes in measuring *boxes* to show dramatic differences in centrosome size. *A: left box*, cytoplasmic pericentrin; *right box*, centrosomal pericentrin. *B: left box*, centrosomal pericentrin; *right box*, cytoplasmic pericentrin. *C* and *D*, an average of eight measurements of centrosomal and cytoplasmic pericentrin in nontumor (*Normal*) and tumor tissues, respectively. Centrosome size (*E*) and number (*F*, normalized to nuclei) were determined as described in "Materials and Methods." Each column in *E* and *F* represents the average of >100 measurements taken from one tumor. *P*s in *C–F* were obtained by paired Student's *t* test. *Bars*, SE.

centrosome antigens immunoreactive to pericentrin antibodies (30–32). Antibody was diluted 1:1000 in TBST [50 mM Tris (pH 6.5), 150 mM NaCl, and 0.5% Tween 20], added to sections at room temperature, and incubated for 1 h. Biotinylated secondary antibody (Vector Laboratories, Burlingame, CA) was applied in TBST for 1 h and amplified by the avidin-biotin-complex method as described (ABC; Vector Laboratories, Burlingame, CA). To block endogenous biotin- and avidin-binding sites, sections were treated with a solution of biotin, followed by a solution of avidin before application of the primary antibody. To avoid nonspecific binding by primary and secondary antibodies, washing solutions contained 5% w/v BSA and 5% v/v goat serum. Endogenous peroxidase was blocked by preincubation in a solution of 3% H_2O_2. After immunostaining, sections were lightly counterstained in hematoxylin.

Criteria for Centrosome Defects. We considered centrosomes abnormal if they had a diameter at least twice that of centrosomes in normal prostate gland epithelium, if they were present in numbers >2, and if they were structurally abnormal, as described previously (18). In some cases, we analyzed levels of the centrosome protein pericentrin at centrosomes and in the cytoplasm by quantifying the opacity/translucence of immunoperoxidase staining. Briefly, bright-field immunoperoxidase images of tumor and normal prostate glands taken at ×1000 were digitally color-inverted so the immunoperoxidase product was a bright signal whose luminosity was proportional to the intensity of the original brown signal. Signals were measured as the integral of a 5-μm area about five times the size of a centrosome, as delineated with the marquee function of Photoshop. Signal emanating from the neighboring cytoplasm was subtracted from the respective centrosome measurement. For cytoplasmic pericentrin measurements, background signals emanating from nontissue sources were subtracted. Inclusion of internal controls (normal glands present within the same section) allowed us to obtain semiquantitatively measurements of pericentrin levels within and between tumors. This approach has been used to establish differences in protein levels of other proteins (33). Members of our Biostatistics core (Dr. Chung Cheng, University of Massachusetts Medical School) performed statistical analysis.

***In Situ* Hybridization with Chromosome-specific Centromere Probes.** For *in situ* hybridization studies, tissue sections parallel to those stained for centrosomes were deparaffinized and heated in a microwave pressure cooker for 20 min in a solution containing 0.01 M sodium citrate (pH 6.0). After cooling to room temperature, sections were treated with a solution of pepsin (40 μg/ml) in 0.1 N HCl for 10 min. Pepsin digestion was stopped by washing the sections several times in 2× SSC at room temperature, and slides were dehydrated in a series of alcohols and air-dried. Biotinylated probes to the centromeric regions of chromosomes 1 or 8 were added in hybridization buffer, and slides were mounted, sealing coverslips with rubber cement. Target DNA and probes were codenatured in a Hybrite oven (Vysis, Downers Grove, IL; Ref. 18), and slides were washed several times in SSC buffers for maximum stringency (Vysis), processed to detect signals (NEN Life Science Products, Boston, MA), and lightly counterstained with hematoxylin to reveal nuclei. Data are shown for chromosome 8 (Figs. 5 and 7) and is similar to that observed with probes to chromosome 1 (not shown).

A total of 100–120 nuclei in tumor and nontumor areas of the section (identified by hematoxylin counterstain) were scored for centromere signals. CIN[3] was determined by computing the fraction of cells with signals greater than the mode (34), a parameter known to underestimate the true CIN level (18, 34). To avoid the compounding effect of nuclear truncation artifact in tissue sections, we computed only chromosome gains. Cells in the G_2 phase of the cell cycle, which normally have four copies of each chromosome, were distinguishable from cells with supernumerary chromosomes because sister chromosomes (and centromere signals) in these cells occur in pairs.

Pericentrin Transfections into Normal or Tumor-derived Prostate Cell Lines. Full length HA-tagged pericentrin in pcDNA I (2 μg; Ref. 32; Invitrogen) was used for transient transfection (Lipofectamine; Life Technologies, Inc., Gaithersburg, MD) of the 1542-NPTX cell line derived from normal prostate epithelium by transformation with E6 and E7 from human papillomavirus type 16 (35). Cells transfected with vector alone served as controls. Permanent pericentrin-expressing PC-3 cells were constructed by cloning full-length HA-pericentrin into the pRetroON vector (Clontech), which codes for a reverse tetracycline transactivator protein and contains tetracycline transactivator responsive elements that drive transcription of the gene of interest. The transactivator is reported to bind and activate the promoter in the presence of tetracycline/doxycycline. After sequence confirmation, the cDNA was introduced into PC-3 cells (American Type Culture Collection) by transient transfection (as above), and 24 permanent lines were obtained after antibiotic selection (Clontech); cell lines expressing vector alone served as controls. We found that HA-pericentrin in these lines was expressed in the absence of doxycycline and did not significantly increase in the presence of doxycycline. The pericentrin-expressing cells exhibited dramatically different features than control cells in the absence of the drug; these features did not noticeably increase in the presence of drug, and they were indistinguishable from features observed in transiently transfected 1542 NPTX cells (Fig. 6) and COS cells (32). Protein expression in the absence of induction from the pRetroON vector and the lack of inducibility of the vector has been noted by Clontech,[4] and they have discontinued its sale. Imperfections in the inducibility of the vector did not impact on our study because we obtained several permanent pericentrin-expressing cell lines. In this study, we present data from cells treated with doxycycline for 48 h.

Immunofluorescence Analysis of Cell Lines. Pericentrin-expressing 1542 NPTX cells (48 h after transfection) and PC-3 cells were fixed in cold

[3] The abbreviations used are: CIN, chromosomal numerical instability; HA, hemagglutinin antigen.

[4] Personal communication.

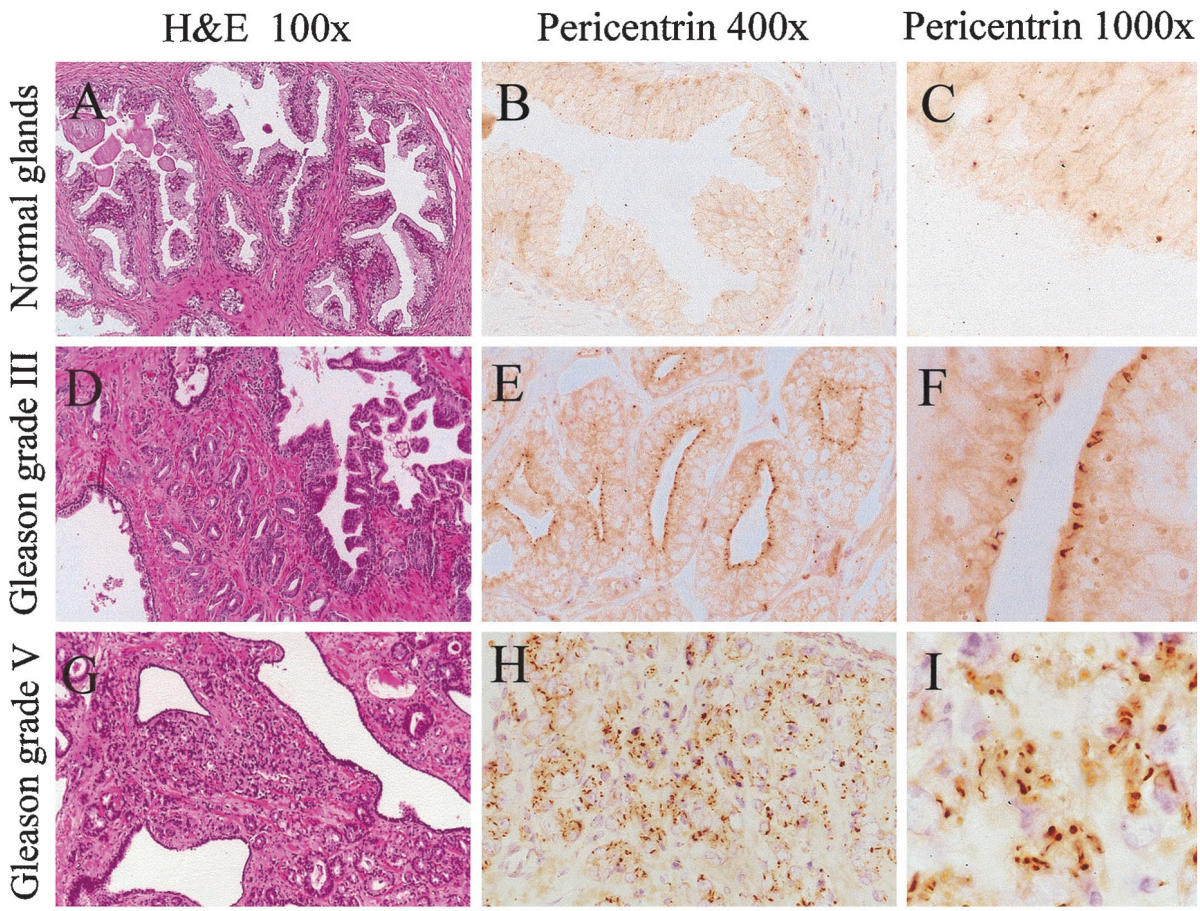

Fig. 3. Centrosome abnormalities increase with increasing Gleason grade: pictorial view. Histological features of a normal prostate gland (*A*) and prostate carcinoma of Gleason grades 3 (*D*) and 5 (*G*) on H&E-stained sections are shown. Areas similar to those imaged in the *left column* were stained for pericentrin at ×400 (*B*, *E*, and *H*) and ×1000 (*C*, *F*, and *I*). With advancing Gleason grade, centrosomes become progressively larger, structurally more abnormal, and greater in number.

methanol and costained for γ-tubulin to label centrosomes and HA to locate transfected cells (1542 NPTX) as described (32). DNA was stained with 4′,6-diamidino-2-phenylindole, and levels were quantified as described (32).

Growth in Agarose of Prostate Cell Lines Permanently Expressing Pericentrin. To study the *in vitro* behavior of cells with deregulated expression of pericentrin, we used the agarose colony assay of Bishop with minor modifications (36). One hundred thousand HA-pericentrin-expressing cells or empty vector cells were plated in duplicate in six-well plates in 0.35% low-melting point agarose over a cushion of 0.7% agarose. Cells were fed full growth medium (10% FCS, 90% RPMI, plus antibiotics and glutamine) and assessed for growth at 3 and 7 days using an inverted microscope equipped with a film camera. Images were then taken at ×40, and colonies were counted and sized after an additional ×10 projection onto a screen. A total of 10 images/cell line were analyzed (between 500 and 1000 colonies).

RESULTS

Centrosome Abnormalities in Prostate Carcinoma. In this study, we analyzed prostate tumors of different cytological grades for the presence of centrosome defects. We selected the area with the highest Gleason grade within each radical prostatectomy, because this parameter appears to be the single most important determinant of clinical outcome (12). We avoided the breakdown of data by Gleason score, as customarily done in clinical data representations, because it represents a compound measure of multiple Gleason grades and may thus obscure the significance of our observations. We examined paraffin sections from radical prostatectomies containing tumors ranging from Gleason grades 2 to 5 ($n = 103$). Gleason grade 1 tumors were not included, because they are rare and relatively difficult to recognize, and because they may have a different ontogenic derivation than more common carcinomas (37). We also analyzed a group of metastatic prostate carcinomas comprised primarily of lymph node and bone marrow metastases ($n = 31$).

Three parameters were initially used to monitor centrosome abnormalities: larger diameter, elevated number, and abnormal structure (Figs. 1 and 2). These parameters were used previously by our group to provide the first evidence for centrosome abnormalities in malignant tumors of multiple tissue origin (18). Analysis of metastatic carcinomas using these criteria demonstrated that all had abnormal centrosomes (31 of 31; Table 1). The proportion of tumor with centrosome defects varied from 15% to virtually 100% of tumor cells. These results confirm our previous results showing that centrosomes are abnormal in prostate tumors (18) and extend these observations to demonstrate that centrosome abnormalities in metastatic tumors appear to be universally present and severe. The majority of carcinomas confined to the prostate (Gleason grades 2–5) also had abnormal centrosomes (101 of 109, Table 1; Fig. 1). However, abnormalities in this heterogeneous group of tumors were more variable than those observed in metastatic carcinomas. Some exhibited defects in only one or two of the three parameters, and the proportions of tumor tissue with centrosome abnormalities were generally lower than in metastatic tumors. In no instance did we observe centrosome abnormalities in nontumor tissues adjacent to tumors (Table 1; Fig. 1).

We reasoned that variability in centrosome defects in this heterogeneous mix of tumors might reflect differences in biological behavior and Gleason grade. To test this, we analyzed six cases each of

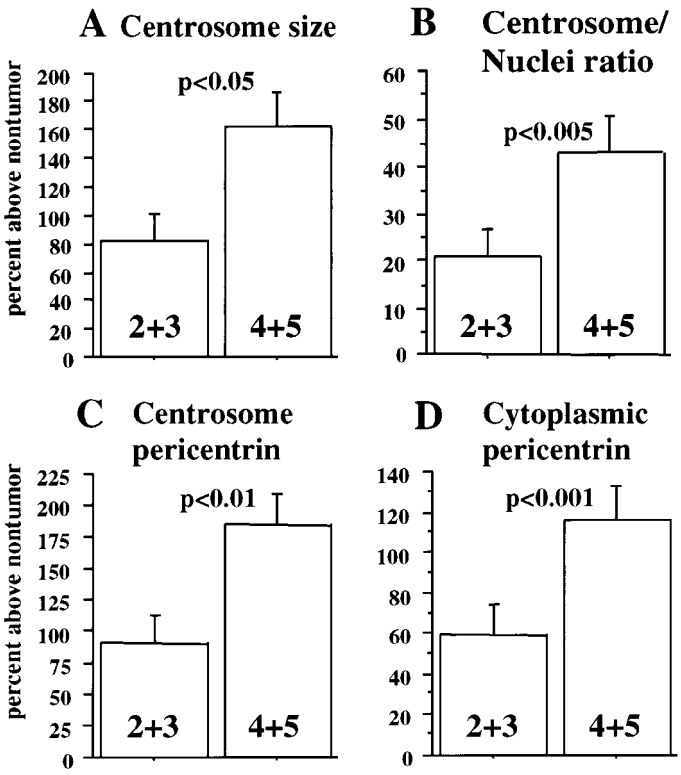

Fig. 4. Centrosome abnormalities and pericentrin levels increase with increasing Gleason grade: quantitative analysis. Centrosome diameter (*A*), centrosome number (centrosome:nuclei ratio, *B*), centrosomal pericentrin (*C*), and cytoplasmic pericentrin (*D*) were determined as described in "Materials and Methods." The *first column* in *A–D* represents the mean of measurements made on six tumors of grade 2 and six of grade 3 combined; the *second column*, similar numbers of grades 4 and 5. All values, a percentage increase above nontumor cells present within the tissue sections (*Y axis*). The data demonstrate that abnormal centrosome features are statistically greater in tumors of higher Gleason grade. *P*s obtained by paired Student's *t* test. *Bars*, SE.

tumors with Gleason grades 2 through 5 for the three parameters of centrosome defects. In addition, we examined in detail the distribution and levels of pericentrin, a highly conserved integral centrosome protein involved in centrosome and spindle organization and chromosome segregation (30–32). Because our previous work had strongly suggested that levels of the centrosome protein pericentrin were higher in tumor *versus* nontumor tissues (18), we analyzed pericentrin levels using a quantitative method established for tissues processed for immunohistochemistry (Ref. 33; Fig. 2, *C* and *D*). Of the five parameters measured, four were significantly higher in tumors of high Gleason grades (combined 4 and 5) compared with those of low Gleason grades (combined 2 and 3; Figs. 3 and 4). Centrosome size and number were 2-fold higher in tumors of high Gleason grade (Fig. 4, *A* and *B*), and pericentrin levels at the centrosome and in the cytoplasm were significantly higher in high-grade tumors (Fig. 4, *C* and *D*). In contrast, neither the severity nor prevalence of structural abnormalities in centrosomes increased with higher Gleason grade (data not shown). Among the structural defects were elongated centrosomes (length:width ratio >5; Figs. 1*E* and 3*I*) that were never observed in normal human prostate cells. This suggested that elongated centrosomes were tumor specific and had potential to serve as a diagnostic marker (see "Discussion"). For all five categories of centrosome defects, the distribution within tumors was somewhat heterogeneous, a pattern reminiscent of that reported for tumor DNA content (38–41).

Relationship between Centrosome Abnormalities and Chromosomal Instability. Because centrosomes play a role in the maintenance of genomic stability through control of mitotic chromosome segregation, we asked if there was a correlation between abnormal centrosomes and genomic instability, specifically CIN. CIN, as first described by Lengauer *et al.* (34), is a measure of the nonmodal distribution of chromosomes that is thought to result from persistent missegregation of chromosomes during mitosis. In this study, we examined the nonmodal distribution of chromosome 8 in prostate tumors of different Gleason grades using centromere-specific nucleotide probes and *in situ* hybridization (see "Materials and Methods" and Fig. 5). As expected, the extent of CIN in tumor tissues was significantly greater than in nontumor tissues (Fig. 5). Interestingly, the extent of CIN was significantly greater in Gleason grade 4/5 than in Gleason grade 2/3 (Fig. 5*C*). Finally, the extent of CIN correlated with the extent of centrosome abnormalities in parallel sections from the same set of tumors (Fig. 5*D*), suggesting a relationship between centrosome defects and genomic instability in prostate tumor progression.

Induction of Centrosome Defects in Prostate Cells by Ectopic Expression of the Centrosome Protein Pericentrin Induces a Prostate Tumor-like Phenotype. If elevated pericentrin levels and centrosome defects observed in prostate tumor tissues contribute to cellular and genetic changes that occur during tumor progression, they may have the potential to induce similar changes when experimentally induced in cultured cells. To directly test this idea, we induced centrosome defects in prostate cells *in vitro*. We expressed a HA-tagged pericentrin protein in cell lines derived from normal prostate epithelium (1542-NPTX; Ref. 35) and from metastatic prostate cancer (PC-3) both by transient transfection and by construction of permanent cell lines (Figs. 6 and 7).

Elevation of pericentrin levels induced or exacerbated genetic instability and cellular changes in 1542-NPTX and PC-3 cells, respectively. 1542-NPTX cells transiently transfected with the HA-pericentrin construct exhibited numerous defects in centrosome size, shape, and number (Fig. 6*E*) as revealed by immunofluorescence staining for the centrosome protein γ-tubulin (42). Defective centrosomes were usually associated with structurally disorganized mitotic spindles, and chromosomes associated with these abnormal spindles were often misaligned and missegregated, indicating that the cells were undergoing aberrant mitoses (data not shown). Consistent with this idea were dramatic changes in nuclear morphology observed in interphase cells (lobate and misshapen nuclei, micronuclei, and multiple nuclei). Moreover, DNA levels were elevated in a large proportion of HA-pericentrin cells but not in control cells, demonstrating that pericentrin expression induced aneuploidy/polyploidy (Fig. 6, *B–D*). Control cells included cells transfected with vector alone (Fig. 6), a truncated pericentrin construct (43) and β-galactosidase (data not shown). Similar results were observed in green fluorescent protein-pericentrin transfected cells (data not shown), indicating that this phenotype was attributable to pericentrin overexpression and unrelated to the expression tag. These studies demonstrate that tumor-like changes in cellular architecture and genetic composition can take place within one to three cell cycles after HA-pericentrin expression.

To examine the long-term effects of HA-pericentrin expression, we constructed permanent prostate tumor-derived cell lines (PC-3; see "Materials and Methods"). The pericentrin-expressing PC-3 cell lines (total, 24) exhibited several abnormal features compared with control PC-3 cells containing empty vector (Fig. 7). Six cell lines were examined in detail, and all gave a similar phenotype; below we present data from one line (PeriPC-3–4.1). The presence of the HA-pericentrin construct was confirmed by PCR analysis (data not shown), and the HA-tagged pericentrin protein was detected by Western blot (Fig. 7*A*). Defects in centrosomes, spindles, and nuclei were significantly higher than in control cells and were strikingly similar to defects observed in transiently transfected 1542-NPTX cells (Fig. 6)

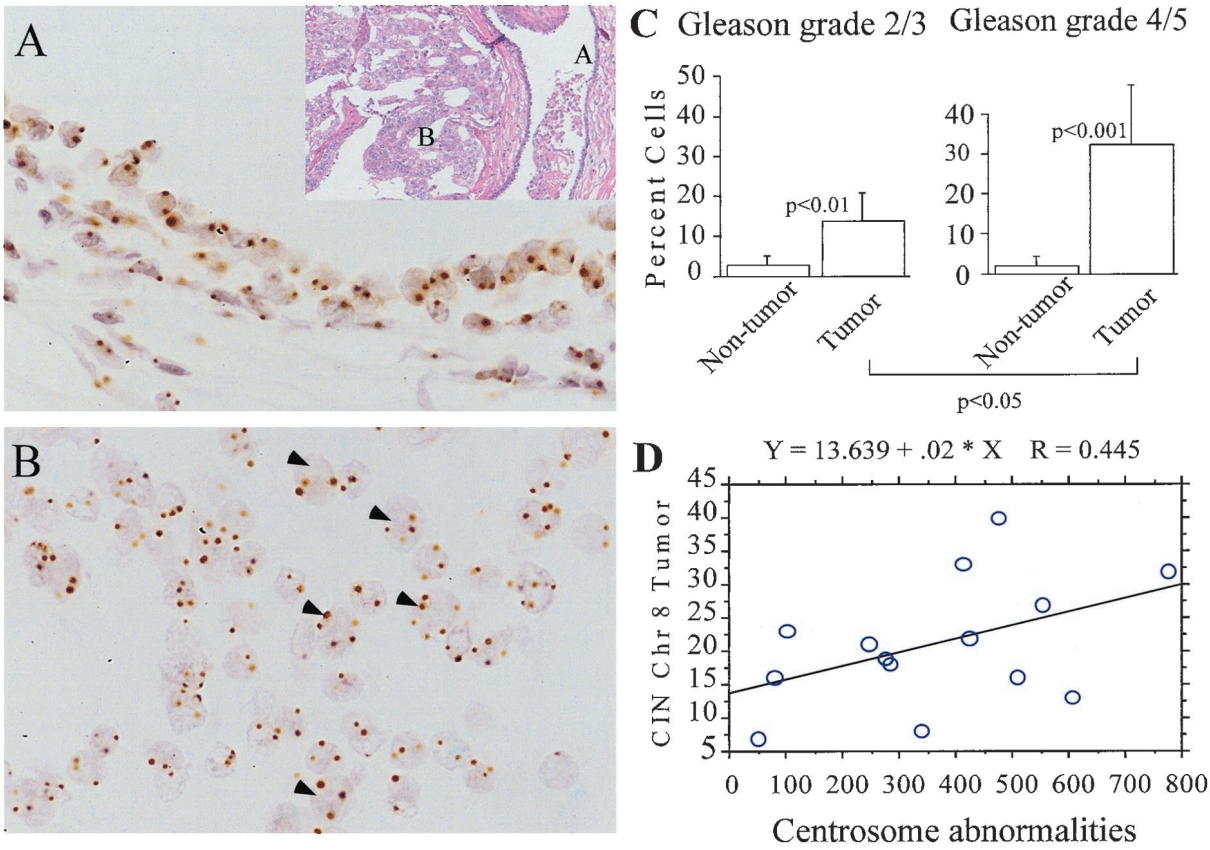

Fig. 5. Chromosome instability increases with increasing Gleason grade in invasive prostate carcinoma. *In situ* hybridization with a chromosome 8-specific centromeric probe in a normal gland (*A*) and Gleason grade 4 prostate carcinoma (*B*). *Inset* in *A*, a low-power (×40) view of an H&E-stained parallel section showing a normal gland (*A*) and high-grade prostate carcinoma (*B*). The figure shows that significant numbers of tumor cells have greater than three signals/nuclei (*B, arrowheads*), whereas no cell shows more than two signals in the normal epithelium (*A*). The extent of CIN (as the fraction of cells with chromosome 8 copy number >2) is greater in tumors of combined Gleason grades 4 and 5 than those of Gleason grades 2 and 3 (*C*) and correlates with the cumulative extent of centrosome abnormalities (*D*, correlation coefficient, $r = 0.445$). *Bars*, SE.

and in prostate tumors (Figs. 1 and 2). DNA content analyzed by flow cytometry (Fig. 7, *E* and *F*) and chromosomal instability assayed by *in situ* hybridization with centromere probes for chromosome 8 (Fig. 7, *C* and *D*) were significantly higher in pericentrin-expressing PC-3 cells. Moreover, the cellular architecture of pericentrin-PC-3 cells was dramatically altered (Fig. 7, *G* and *H*), and the cells grew more rapidly in soft agar compared with controls (Fig. 7, *I–K*). Taken together, these data demonstrate that expression of a single centrosome protein in normal and prostate tumor cells can induce or exacerbate abnormalities in centrosome number and structure, cellular architecture, nuclear morphology, cell growth, and genomic stability, features that are characteristically altered in aggressive prostate tumors.

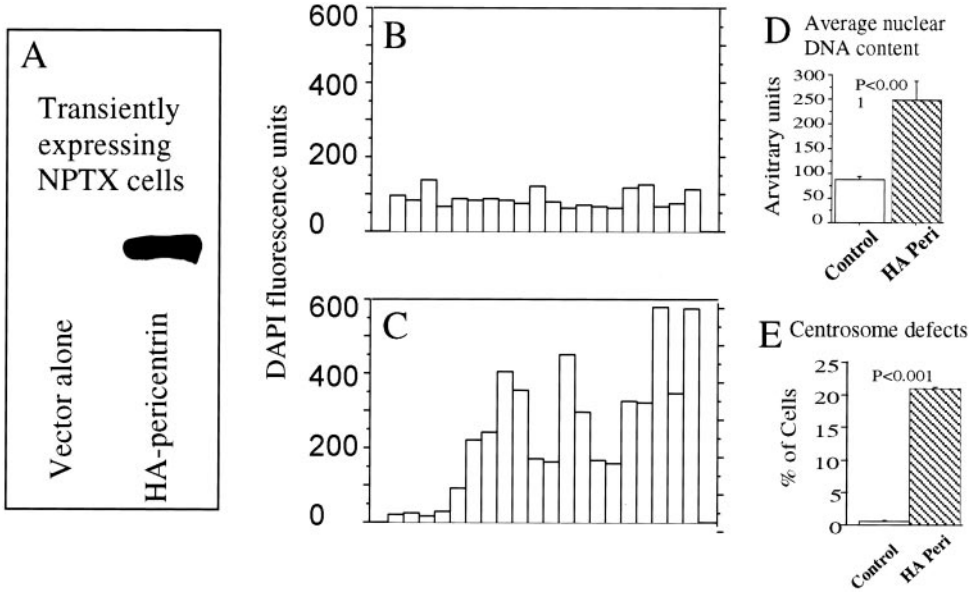

Fig. 6. Transient expression of pericentrin in "normal" near-diploid prostate cells induces centrosome defects, nuclear abnormalities, and aneuploidy. 1542-NPTX cells were transfected with the HA-pericentrin construct or vector alone and grown for an additional 40 hours. *A*, Western blot after immunoprecipitation of HA-pericentrin from cell lysates. Microspectrofluorometric quantification of DNA stained with 4′,6-diamidino-2-phenylindole shows that most HA-pericentrin-expressing cells (*C*) had higher or lower nuclear DNA content than control cells (*B*). The average nuclear DNA content of individual cells (*D*, >100 cells/column). *Bars*, SE. Centrosome defects detected in cells stained for γ-tubulin were >20-fold higher in HA-pericentrin-expressing cells (*E*).

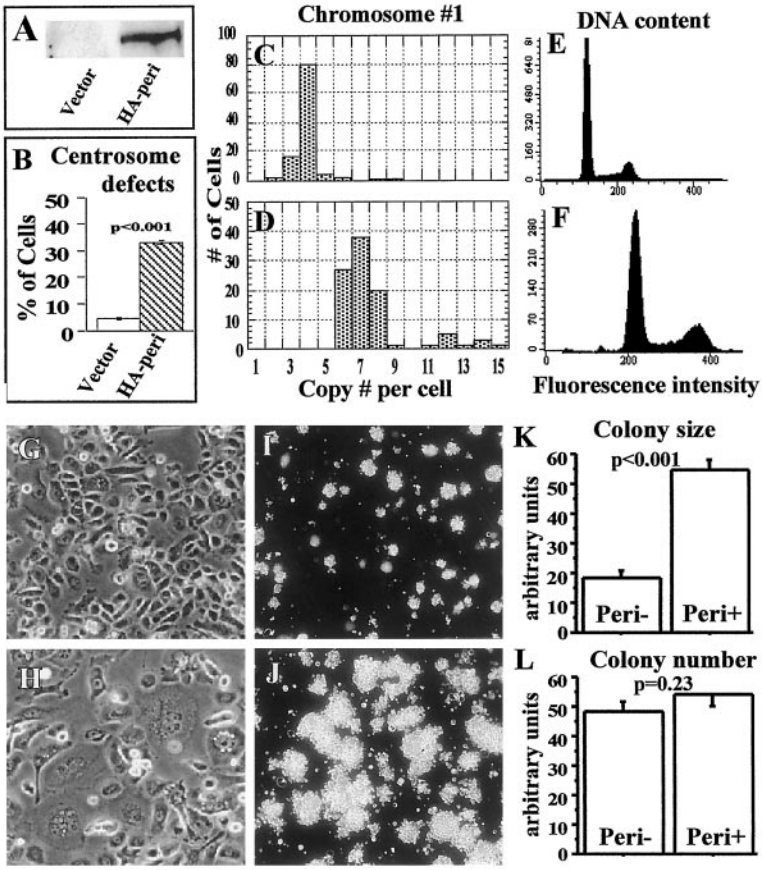

Fig. 7. Permanent prostate tumor cell lines expressing pericentrin have tumor-like features. *A*, Western blot after immunoprecipitation of HA-pericentrin from cell lysates. Centrosome defects were detected and quantified as described in Fig. 6*B*. *In situ* hybridization with centromere probes to chromosome 8 to evaluate chromosome instability (*C* and *D*) or with propidium iodide to determine DNA content by flow cytometry (*E* and *F*) is shown. *Y axis*, propidium iodide fluorescence. Changes in cellular architecture are observed in HA-pericentrin cells (*H*) compared with controls (*G*, note larger cells with larger nuclei). HA-pericentrin-expressing cells exhibit enhanced growth in agarose (*J*) compared with controls (*I*), as shown by a significant increase in colony size (*K*, *Peri+*) but not number (*L*, *Peri+*).

DISCUSSION

The results presented here demonstrate that centrosomes are structurally and numerically abnormal in the vast majority of metastatic and invasive prostate carcinomas. These abnormalities are frequent and usually occur together in the same tumor. The extent of centrosome abnormalities in invasive prostate carcinoma correlates with the Gleason grade in that tumors with the highest Gleason grade have more extensive centrosome abnormalities. The extent of chromosome instability correlates with the extent of centrosome abnormalities, both increasing with increasing Gleason grade. These observations are consistent with the idea that centrosome defects contribute to genomic instability during prostate cancer progression. Support for this idea comes from data showing that artificial induction of centrosome defects by pericentrin overexpression can induce genetic instability, loss of cellular architecture, and rapid cell growth in prostate cells.

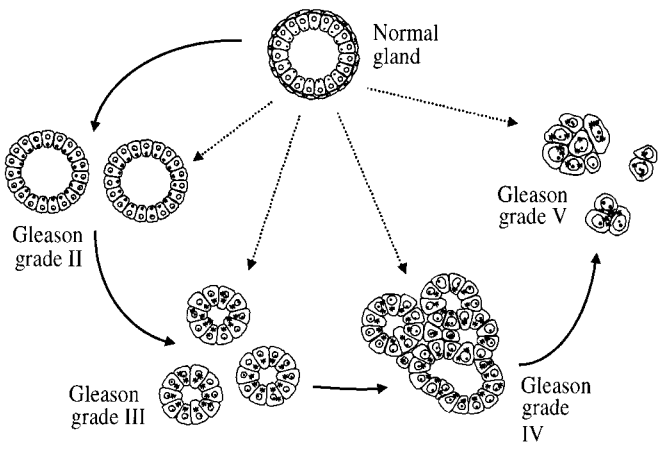

Fig. 8. Centrosome-based model for prostate cancer progression. Diagram of normal (*above*) and neoplastic prostate glands (*below*) showing the most salient cytoarchitectural features of tumors with increasing Gleason grade. In our model, centrosomes (*) become increasingly abnormal and misallocated during tumor progression, concurrent with abnormalities in nuclei and nucleoli (*filled dot*), cellular and glandular disorganization, and chromosome instability. *Filled arrows*, currently favored evolutionary pathways; *segmented arrows*, possible alternative pathways. Neither pathway has been convincingly demonstrated for prostate carcinoma. Gleason grade I and prostatic intraepithelial neoplasm lesions are not represented.

The *in vivo* and *in vitro* data presented in this report implicate centrosomes in the progression of prostate cancer. In our current model (Fig. 8), centrosome dysfunction causes modification of the microtubule cytoskeleton and contributes directly to cellular and glandular disorganization and genomic instability, creating cells that are predisposed to additional changes that lead to aggressive tumor development. We do not know whether centrosome abnormalities develop in a progressive manner (Fig. 8, *solid arrow*) or in a discontinuous fashion (Fig. 8, *segmented arrows*). Elucidation of the mechanisms by which centrosome changes occur may provide insights into the evolutionary pathway of the cytoarchitectural features that occur during prostate cancer progression (44, 45).

Our observations of CIN in prostate carcinoma are consistent with those made previously by Lengauer *et al.* (34) in colon carcinoma cells, and they suggest that CIN may be the most important cause of aneuploidy in colon and prostate tumors. Because centrosome abnormalities are found in essentially all carcinomas examined to date (18), they may be a major cause of aneuploidy/CIN in solid tumors (18, 46). Consistent with this idea are data implicating centrosome dysfunction in CIN and aneuploidy in colon carcinoma cell lines (47).

Our work has important implications for prostate cancer progression,

prognosis, and treatment. Our observations suggest that progressive dysfunction of centrosomes occurs in prostate carcinoma, and that this can have far-reaching effects on cell morphology and genetic composition. Elucidating the mechanism(s) that leads to centrosome dysfunction in prostate carcinoma and the fundamental differences between centrosomes of low- and high-grade tumors could lead to the development of markers for tumor virulence. Such markers could play a critical role in identifying the subset of patients destined to develop aggressive, lethal prostate carcinoma. For example, elevated levels of centrosome proteins could provide a potential marker for early prostate lesions. If released into the circulation like prostate-specific antigen, these proteins could provide a noninvasive method to detect early lesions that lead to aggressive disease. Centrosome abnormalities also constitute an attractive, novel therapeutic target because they are tumor specific. It may be possible to develop chemical inhibitors against molecular components of centrosomes, such as pericentrin, that could correct or reverse centrosome defects, genetic instability, and tumor progression.

ACKNOWLEDGMENTS

We thank Dr. G. Stein and G. Sluder (Department of Cell Biology) for critical reading of the manuscript and Dr. C. Hsieh (Biostatistics Core Facility, University of Massachusetts Cancer Center) for assistance with statistical analysis.

REFERENCES

1. Greenlee, R. T., Murray, T., Bolden, S., and Wingo, P. A. Cancer statistics, 2000. CA Cancer J. Clin., *50:* 7–33, 2000.
2. Merrill, R. M., Weed, D. L., and Feuer, E. J. The lifetime risk of developing prostate cancer in white and black men. Cancer Epidemiol. Biomark. Prev., *6:* 763–768, 1997.
3. Miller, B., Ries, L., and Hankey, B. Cancer Statistics Review: 1973–1989, NIH publication 92-2789, Bethesda, MD: Department of Health and Human Services, 1992.
4. Seidman, H., Mushinski, M. H., Gelb, S. K., and Silverberg, E. Probabilities of eventually developing or dying of cancer–United States, 1985. CA Cancer J. Clin., *35:* 36–56, 1985.
5. Silverberg, E. Statistical and epidemiologic data on urologic cancer. Cancer (Phila.), *60:* 692–717, 1987.
6. Bostwick, D. G., Cooner, W. H., Denis, L., Jones, G. W., Scardino, P. T., and Murphy, G. P. The association of benign prostatic hyperplasia and cancer of the prostate. Cancer (Phila.), *70:* 291–301, 1992.
7. Fowler, F. J., Jr., McNaughton Collins, M., Albertsen, P. C., Zietman, A., Elliott, D. B., and Barry, M. J. Comparison of recommendations by urologists and radiation oncologists for treatment of clinically localized prostate cancer. J. Am. Med. Assoc., *283:* 3217–3222, 2000.
8. Wilt, T. J. Uncertainty in prostate cancer care: the physician's role in clearing the confusion. J. Am. Med. Assoc., *283:* 3258–3260, 2000.
9. von Eschenbach, A. The challenge of prostate cancer. CA Cancer J. Clin., *49:* 262–263, 2000.
10. Gleason, D. F. Classification of prostatic carcinomas. Cancer Chemother. Rep., *50:* 125–128, 1966.
11. Gleason, D. F., and Mellinger, G. T. Prediction of prognosis for prostatic adenocarcinoma by combined histological grading and clinical staging. J. Urol., *111:* 58–64, 1974.
12. Stamey, T. A., McNeal, J. E., Yemoto, C. M., Sigal, B. M., and Johnstone, I. M. Biological determinants of cancer progression in men with prostate cancer. J. Am. Med. Assoc., *281:* 1395–1400, 1999.
13. Dejter, S. W., Jr., Cunningham, R. E., Noguchi, P. D., Jones, R. V., Moul, J. W., McLeod, D. G., and Lynch, J. H. Prognostic significance of DNA ploidy in carcinoma of prostate. Urology, *33:* 361–366, 1989.
14. Frankfurt, O. S., Chin, J. L., Englander, L. S., Greco, W. R., Pontes, J. E., and Rustum, Y. M. Relationship between DNA ploidy, glandular differentiation, and tumor spread in human prostate cancer. Cancer Res., *45:* 1418–1423, 1985.
15. Greene, D. R., Taylor, S. R., Wheeler, T. M., and Scardino, P. T. DNA ploidy by image analysis of individual foci of prostate cancer: a preliminary report. Cancer Res., *51:* 4084–4089, 1991.
16. Hussain, M. H., Powell, I., Zaki, N., Maciorowski, Z., Sakr, W., KuKuruga, M., Visscher, D., Haas, G. P., Pontes, J. E., and Ensley, J. F. Flow cytometric DNA analysis of fresh prostatic resections. Cancer (Phila.), *72:* 3012–3019, 1993.
17. Scrivner, D. L., Meyer, J. S., Rujanavech, N., Fathman, A., and Scully, T. Cell kinetics by bromodeoxyuridine labeling and deoxyribonucleic acid ploidy in prostatic carcinoma needle biopsies. J. Urol., *146:* 1034–1039, 1991.
18. Pihan, G. A., Purohit, A., Wallace, J., Knecht, H., Woda, B., Quesenberry, P., and Doxsey, S. J. Centrosome defects and genetic instability in malignant tumors. Cancer Res., *58:* 3974–3985, 1998.
19. Kellogg, D. R., Moritz, M., and Alberts, B. M. The centrosome and cellular organization. Annu. Rev. Biochem., *63:* 639–674, 1994.
20. Zimmerman, W., Sparks, C. A., and Doxsey, S. J. Amorphous no longer: the centrosome comes into focus. Curr. Opin. Cell Biol., *11:* 122–128, 1999.
21. Bornens, M. Cell polarity: intrinsic or externally imposed? New Biol., *3:* 627–636, 1991.
22. Meads, T., and Schroer, T. A. Polarity and nucleation of microtubules in polarized epithelial cells. Cell Motil. Cytoskeleton, *32:* 273–288, 1995.
23. Rizzolo, L. J., and Joshi, H. C. Apical orientation of the microtubule organizing center and associated γ-tubulin during the polarization of the retinal pigment epithelium *in vivo*. Dev. Biol., *157:* 147–156, 1993.
24. Whitehead, C. M., and Salisbury, J. L. Regulation and regulatory activities of centrosomes. J. Cell. Biochem., *32–33* (Suppl.)*:* 192–199, 1999.
25. Brown, C. R., Hong-Brown, L. Q., Doxsey, S. J., and Welch, W. J. Molecular chaperones and the centrosome. J. Biol. Chem., *271:* 833–840, 1996.
26. Pines, J. Four-dimensional control of the cell cycle. Nat. Cell Biol. *1:* E73–E79, 1999.
27. Pockwinse, S. M., Krockmalnic, G., Doxsey, S. J., Nickerson, J., Lian, J. B., van Wijnen, A. J., Stein, J. L., Stein, G. S., and Penman, S. Cell cycle independent interaction of CDC2 with the centrosome, which is associated with the nuclear matrix-intermediate filament scaffold. Proc. Natl. Acad. Sci. USA, *94:* 3022–3027, 1997.
28. Raff, J. W. The missing (L) UNC? Curr. Biol., *9:* R708–R710, 1999.
29. Sluder, G., and Hinchcliffe, E. H. Control of centrosome reproduction: the right number at the right time. Biol. Cell, *91:* 413–427, 1999.
30. Doxsey, S. J., Stein, P., Evans, L., Calarco, P. D., and Kirschner, M. Pericentrin, a highly conserved centrosome protein involved in microtubule organization. Cell, *76:* 639–650, 1994.
31. Dictenberg, J. B., Zimmerman, W., Sparks, C. A., Young, A., Vidair, C., Zheng, Y., Carrington, W., Fay, F. S., and Doxsey, S. J. Pericentrin and γ-tubulin form a protein complex and are organized into a novel lattice at the centrosome. J. Cell Biol., *141:* 163–174, 1998.
32. Purohit, A., Tynan, S. H., Vallee, R., and Doxsey, S. J. Direct interaction of pericentrin with cytoplasmic dynein light intermediate chain contributes to mitotic spindle organization. J. Cell Biol., *147:* 481–492, 1999.
33. Matkowskyj, K. A., Schonfeld, D., and Benya, R. V. Quantitative immunohistochemistry by measuring cumulative signal strength using commercially available software photoshop and matlab. J. Histochem. Cytochem., *48:* 303–312, 2000.
34. Lengauer, C., Kinzler, K. W., and Vogelstein, B. Genetic instability in colorectal cancers. Nature (Lond.), *386:* 623–627, 1997.
35. Bright, R. K., Vocke, C. D., Emmert-Buck, M. R., Duray, P. H., Solomon, D., Fetsch, P., Rhim, J. S., Linehan, W. M., and Topalian, S. L. Generation and genetic characterization of immortal human prostate epithelial cell lines derived from primary cancer specimens. Cancer Res., *57:* 995–1002, 1997.
36. Ziegler, S. F., Levin, S. D., and Perlmutter, R. M. Transformation of NIH 3T3 fibroblasts by an activated form of p59hck. Mol. Cell. Biol., *9:* 2724–2727, 1989.
37. Grignon, D. J., and Sakr, W. A. Zonal origin of prostatic adenocarcinoma: are there biologic differences between transition zone and peripheral zone adenocarcinomas of the prostate gland? J. Cell. Biochem. Suppl., *19:* 267–269, 1994.
38. Irinopoulou, T., Vassy, J., Beil, M., Nicolopoulou, P., Encaoua, D., and Rigaut, J. P. Three-dimensional, DNA image cytometry by confocal scanning laser microscopy in thick tissue blocks of prostatic lesions. Cytometry, *27:* 99–105, 1997.
39. Irinopoulou, T., Vassy, J., and Rigaut, J. P. Application of confocal scanning laser microscopy to 3-D DNA image cytometry of prostatic lesions. Anal. Quant. Cytol. Histol., *20:* 351–357, 1998.
40. Petein, M., Michel, P., van Velthoven, R., Pasteels, J. L., Brawer, M. K., Davis, J. R., Nagle, R. B., and Kiss, R. Morphonuclear relationship between prostatic intraepithelial neoplasia and cancers as assessed by digital cell image analysis. Am. J. Clin. Pathol., *96:* 628–634, 1991.
41. Warzynski, M. J., Soechtig, C. E., Maatman, T. J., Goldsmith, L. C., Grobbel, M. A., Carothers, G. G., and Shockley, K. F. DNA heterogeneity determined by flow cytometry in prostatic adenocarcinoma–necessitating multiple site analysis. Prostate, *27:* 329–335, 1995.
42. Schiebel, E. γ-tubulin complexes: binding to the centrosome, regulation, and microtubule nucleation. Curr. Opin. Cell Biol., *12:* 113–118, 2000.
43. Young, A., Dictenberg, J., Purohit, A., Tuft, R., and Doxsey, S. J. Cytoplasmic dynein-mediated assembly of pericentrin and γ-tubulin onto centrosomes. Mol. Biol. Cell, *11:* 2047–2056, 2000.
44. Epstein, J. I., Carmichael, M. J., Partin, A. W., and Walsh, P. C. Small high grade adenocarcinoma of the prostate in radical prostatectomy specimens performed for nonpalpable disease: pathogenetic and clinical implications. J. Urol., *151:* 1587–1592, 1994.
45. McNeal, J. E. Prostatic microcarcinomas in relation to cancer origin and the evolution to clinical cancer. Cancer (Phila.), *71:* 984–991, 1993.
46. Pihan, G. A., and Doxsey, S. J. The mitotic machinery as a source of genetic instability in cancer. Semin. Cancer Biol., *9:* 289–302, 1999.
47. Ghadimi, B. M., Sackett, D. L., Difilippantonio, M. J., Schrock, E., Neumann, T., Jauho, A., Auer, G., and Ried, T. Centrosome amplification and instability occurs exclusively in aneuploid, but not in diploid colorectal cancer cell lines, and correlates with numerical chromosomal aberrations. Genes Chromosomes Cancer, *27:* 183–190, 2000.